Glyoxal photodissociation. II. An *ab initio* direct classical trajectory study of $C_2H_2O_2 \rightarrow CO+H_2CO$

Xiaosong Li, John M. Millam, and H. Bernhard Schlegel
Department of Chemistry, Wayne State University, Detroit, Michigan 48202

(Received 6 June 2001; accepted 27 July 2001)

Photodissociation of glyoxal via the H_2CO+CO channel has been investigated by *ab initio* classical trajectory calculations using Becke's three-parameter hybrid functional method with split valence and polarized basis set [B3LYP/6-311G(d,p)]. To model the experimental conditions, trajectories were started from a microcanonical ensemble at the transition state with 8.5 kcal/mol excess energy distributed among the vibrational modes and the transition vector. The CO product was produced with a broad rotational distribution but with almost no vibration excitation. When combined with the results from the H_2+2CO channel, the calculated vibrational and rotational distributions of CO are in excellent agreement with the experimental observations. The rotational distribution of H_2CO was very broad ranging up to $J=85$. The H_2CO product has significant vibrational excitation in the out-of-plane bending, CH_2 rocking, CH_2 scissoring, and CO stretching modes. For both the H_2+2CO and the $CO+H_2CO$ channels, the majority of available energy was partitioned into translations. © *2001 American Institute of Physics.* [DOI: 10.1063/1.1404141]

I. INTRODUCTION

Glyoxal has been of interest to both experimentalists and theoreticians for more than two decades.[1–12] In 1980, Parmenter and co-workers presented evidence suggesting that glyoxal dissociated in the absence of collisions.[5] This work was followed by extensive experimental as well as theoretical efforts. It is now generally agreed that under collision-free conditions, there is no observed intersystem crossing to T_1, and the fluorescence quantum yield from S_1 is ca. 50% with the remainder of the glyoxal undergoing internal conversion to S_0 with a high degree of vibrational excitation.[7,8,11,12] The long lifetime of the S_1 state (order of 10^{-6} s)[1,10] provides ample time for vibrational energy redistribution within the energized molecule. Internal conversion from S_1 to S_0 yields an excess energy of 63–65 kcal/mol. With this energy, glyoxal can fragment via three channels:

$$C_2H_2O_2 \rightarrow H_2CO+CO, \quad (1)$$

$$\rightarrow H_2+2CO, \quad (2)$$

$$\rightarrow HCOH+CO. \quad (3)$$

Hepburn *et al.* have measured branching ratios of 9:3.9:1 (channel 1:channel 2:channel 3) for the collisionless fragmentation of glyoxal,[9] indicating that the $C_2H_2O_2 \rightarrow H_2CO+CO$ channel is the most probable. In an early study, Osamura *et al.* reported two transition states for glyoxal photodissociation via $C_2H_2O_2 \rightarrow H_2CO+CO$ channel [Figs. 1(a) and 1(b)].[7] Recent calculations by our group[13] at the CBS-APNO level of theory and by Peslherbe and co-workers[14] at the G3 level of theory show these two structures are 12–20 kcal/mol higher in energy than that for the triple whammy channel, which contrasts sharply with the experimentally observed high fragmentation yield. The correct transition structure for reaction (1) is a 1,2 hydrogen shift across the C–C bond [Fig. 1(c)]. This transition state is 4.8–5.7 kcal/mol lower in energy than that of channel (2),[13,14] in agreement with the higher branching ratio.

Channel (2) has received more attention than channel (1), since it is an unusual unimolecular reaction involving one transition state decomposing into three fragments and, therefore, has been whimsically termed the ''triple whammy'' channel. In an earlier paper[15] we studied this three-body photodissociation of glyoxal by direct *ab initio* trajectory calculations. The H_2 vibrational and rotational states distributions were in good accord with experimental observations. However, since all three channels produce CO as a product, trajectory studies for the other channels are also needed so that the combined vibrational and rotational state distributions for CO can be compared with experiment. Since the $C_2H_2O_2 \rightarrow H_2CO+CO$ channel has the lowest barrier and the highest branching ratio, we have undertaken a direct *ab initio* trajectory study of this channel in the present paper.

II. METHOD

As we have reported in a previous study of the energetics for the glyoxal photodissociation,[13] the most reliable barrier height of glyoxal photodissociation via $C_2H_2O_2 \rightarrow H_2CO+CO$ is calculated to be 54.4 kcal/mol at the CBS-APNO level of theory (see Table III). Experimentally, glyoxal photodissociation occurs after exciting low lying vibrational bands such as 0_0^0, which corresponds to 62.9 kcal/mol energy above the *trans*-glyoxal ground state and 8.5 kcal/mol above the transition state.

In the study of glyoxal photodissociation via the ''triple whammy'' channel, we found that the best agreement with experiment was obtained at the B3LYP level of theory. In the present paper, we continue our study of the dissociation of glyoxal by using direct *ab initio* classical trajectory calculations to investigate the dynamics of the CH_2O+CO channel. The trajectories were started at the transition state and a mi-

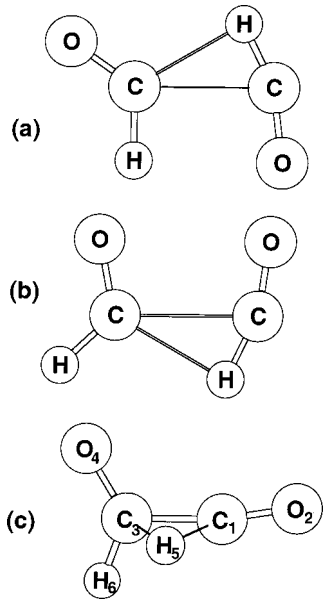

FIG. 1. Optimized geometries of the transition states for glyoxal $\rightarrow H_2CO+CO$.

crocanonical ensemble was constructed distributing $E_{tot}=8.5$ kcal/mol energy among the 11 vibrational normal modes and translation along the transition.[16,17] The total angular momentum was set to zero since the reactant is rotationally cold under experimental conditions. All the possible vibrational states up to 8.5 kcal/mol were generated within the harmonic oscillator approximation. For the motion along the reaction coordinate (i.e., along the transition vector), a uniform distribution of momentum in the direction of the products was used. For a given translational energy along the transition vector, E_{trn}, all vibrational states between $E_{tot}-E_{trn}-\frac{1}{2}\Delta E$ and $E_{tot}-E_{trn}+\frac{1}{2}\Delta E$ were selected; ΔE was adjusted to yield the desired number of states. For the 8.5 kcal/mol microcanonical ensemble with the B3LYP/6-311G(d,p) electronic structure method, $\Delta E=25\,cm^{-1}$ yields 205 states (a detailed list of the initial states is available at http://www.chem.wayne.edu/Schlegel/supp-mat). For a specific vibrational mode with a given number of quanta, the initial phase is chosen randomly. Since the actual potential energy surface is not strictly harmonic, the initial vibrational coordinates and momenta generated by this procedure are scaled to yield the desired vibrational energy.[17] Where appropriate, error bars of one standard deviation are included in the plots.

The trajectories were calculated directly from the electronic structure computations without first fitting a global potential energy surface using the development version of the Gaussian series of programs.[18] A Hessian based method with updating was employed to integrate the trajectories. The Hessian was updated every five steps before being recalculated analytically.[19] A step size of 0.25 amu$^{1/2}$ bohr was used to all of the trajectory calculations. Products were considered totally separated when they were ca. 8 bohr apart or the gradient of the potential between product molecules was less than 1×10^{-5} hartree/bohr. The total energy and total angular momentum were conserved to 10^{-7} hartree and better than $10^{-8}\,\hbar$, respectively. The mass-weighted steepest descent reaction paths were calculated using the method of Gonzalez and Schlegel.[20,21]

To analyze the vibrational energy of the CO product, a Morse function was fit to the potential energies at variant distances. The Morse function was used to obtain the vibrational quantum numbers of the diatomic product by integrating the momentum over one vibration period using the Einstein–Brillouin–Keller (EBK) semiclassical quantization condition.[22,23] For the polyatomic product, the vibrational kinetic energy for each mode was obtained by decomposing the mass-weighted velocity into the instantaneous normal modes. The vibrational potential energy for each mode was estimated by assuming a local harmonic approximation:

$$E_{pot}=\tfrac{1}{2}g_t^2H_{ii}^{-1},$$

where g_i is the gradient and H_{ii} is the Hessian element for the ith instantaneous normal mode. This equation is applicable only if the frequency is not too low and if the potential is not too anharmonic. The lowest frequency of H_2CO is 1202.2 cm^{-1}, corresponding to HCH out-of-plane bending in the equilibrium structure calculated at the B3LYP/6-311+G(d,p) level of theory. The vibrational quantum numbers for each normal mode are obtained from the kinetic and potential energies in the harmonic oscillator approximation.

III. RESULTS AND DISCUSSIONS

A. Structures and energetics

The optimized geometries for the true transition state of channel (1) are shown in Fig. 1(c) and compared in Table I. All levels of theory show a similar structure. At our most reliable level of theory, QCISD/6-311G(d,p), the CC bond length is calculated to be 1.483 Å, compared to 1.530 Å for that of *trans*-glyoxal, demonstrating that the CC bond is intact in the transition state. The migrating hydrogen has moved approximately halfway across the CC bond, and shows CH distances similar to other 1,2 hydrogen shift transition structures. The bond length of the departing CO is

TABLE I. Optimized geometries for transition states.[a]

	CC	C_3O_4	C_1O_2	C_3H_6	C_1H_5	HH	CCO_4	CCO_2	CCH_6	CCH_5	OCCO	HCCH
HF/3-21G	1.485	1.240	1.142	1.082	1.621	1.863	124.4	179.1	106.2	55.0	−104.2	87.7
MP2/6-311G(d,p)	1.487	1.233	1.161	1.101	1.529	1.855	120.9	170.4	109.4	55.1	−20.8	86.4
BH&HLYP/6-311G(d,p)	1.457	1.224	1.135	1.095	1.527	1.843	122.3	175.3	108.8	54.5	−42.4	88.3
B3LYP/6-311G(d,p)	1.472	1.236	1.152	1.100	1.542	1.870	118.7	167.4	111.8	55.3	−17.2	86.4
QCISD/6-311G(d,p)	1.483	1.235	1.154	1.101	1.538	1.869	120.8	171.1	109.7	55.2	−24.3	87.1

[a]Bond lengths in Å, angles in degrees; see Fig. 1 for atom numbering.

TABLE II. Vibrational frequencies for glyoxal minima and transition state.[a]

	ν_1	ν_2	ν_3	ν_4	ν_5	ν_6	ν_7	ν_8	ν_9	ν_{10}	ν_{11}	ν_{12}
trans $C_2H_2O_2$												
HF/3-21G	311	356	601	948	1111	1218	1466	1494	1905	1937	3236	3239
MP2/6-311G(d,p)	149	333	563	836	1079	1098	1351	1398	1745	1759	3007	3012
BH&HLYP/6-311G(d,p)	151	384	584	863	1121	1132	1383	1430	1907	1923	3057	3060
B3LYP/6-311G(d,p)	143	332	552	818	1056	1076	1329	1376	1808	1810	2924	2929
transition state for $C_2H_2O_2 \rightarrow H_2CO+CO$												
HF/3-21G	1327i	233	509	667	856	1049	1360	1414	1526	1625	2229	3221
MP2/6-311G(d,p)	1097i	153	487	636	871	994	1164	1372	1548	1673	2068	3050
BH&HLYP/6-311G(d,p)	1088i	170	502	689	905	1046	1227	1409	1573	1754	2228	3062
B3LYP/6-311G(d,p)	1058i	182	493	637	883	968	1146	1350	1484	1627	2104	2993

[a]Harmonic frequencies in cm^{-1} without scaling.

1.154 Å, which is very close to the CO equilibrium bond length of 1.134 Å, and the corresponding CCO angle is almost linear. Table II lists the frequencies of the transition state at various levels of theory. All levels of theory predict that this structure is a true transition state with one imaginary frequency. Inspection of the normal mode for this vibration confirms that the transition vector corresponds to a 1,2 hydrogen shift. The excellent agreement between the reaction enthalpies computed at the CBS-APNO level and experiment in Table III suggests that the energy barrier of 54.4 kcal/mol for the H_2CO+CO channel should be reliable.

B. Reaction path

Figure 2 shows the potential energy profiles along the mass-weighted steepest descent reaction path (intrinsic reaction coordinate). Similar to that of the triple whammy channel,[15] the potential energy released at the HP/6-311G(d,p) level of theory is about 13 kcal/mol larger than the CBS-APNO value. Both B3LYP/6-311G(d,p) and MP2/6-311G(d,p) predict the energy released within ± 3 kcal/mol of the CBS-APNO result. Notice that there are two distinct slopes in the profile at the HP/6-311G(d,p) and MP2/6-311G(d,p) levels of theory. Calculations show that the slope near the transition state corresponds to the energy release accompanying the 1,2 hydrogen shift. In this region, the CC bond breaking process is very slow with an elongation of ca. 0.15 Å. When the hydrogen shift is nearly complete, the C–C bond breaking proceeds rapidly with a steeper slope toward products. The potential energy profile at the B3LYP/6-311G(d,p) level is smoother, indicating a similar rate of energy release for the 1,2 hydrogen shift and the C–C bond breaking. The reaction path following calculations show the transition between these two phases of the reaction is near $s=1.5\,\mathrm{amu}^{1/2}\,\mathrm{bohr}$. The molecular geometry at this point is illustrated in Fig. 3. As can be seen, the hydrogen shift has finished and the products are beginning to separate. The CO product bond length is 1.134 Å at the MP2/6-311G(d,p) level, and about 25%–29% potential energy has been released, compared to 27%–34% for channel (2) at $s=1.0\,\mathrm{amu}^{1/2}\,\mathrm{bohr}$ where the H_2 bond formation is 80%–90% complete.

TABLE III. Reaction enthalpies and barrier heights.[a]

	$\Delta H^{\circ}_{r,298}$	ΔH^{I}_{298} forward
HF/3-21G	−7.6	78.0
HF/6-311G(d,p)	−12.9	67.8
MP2/6-311G(d,p)	−5.3	56.6
BH&HLYP/6-311G(d,p)	−1.4	59.1
B3LYP/6-311G(d,p)	−0.2	51.6
CBS-APNO	−1.4	54.4
experiment	-1.8 ± 0.2	

[a]Enthalpies at 298 K in kcal/mol, experimental data from Ref. 25.

C. Dynamics

The average time for glyoxal dissociation via the $C_2H_2O_2 \rightarrow H_2CO+CO$ channel is ca. 100 fs, compared to 50–55 fs for the $C_2H_2O_2 \rightarrow H_2+2CO$ channel. The longer dissociation time for H_2CO+CO is due to the slow hydrogen shift process. Inspection of the trajectory shows that the first 35–40 fs of the reaction corresponds to the hydrogen shift, with the remaining time associated with the elongation of the CC bond and separation of the products. The calculated impact parameter for $C_2H_2O_2 \rightarrow H_2CO+CO$ is about 0.56, compared to 0.98 for the formaldehyde photodissociation.[24]

Figure 4 shows the calculated translational energy distributions for CO and H_2CO produced from the H_2CO+CO

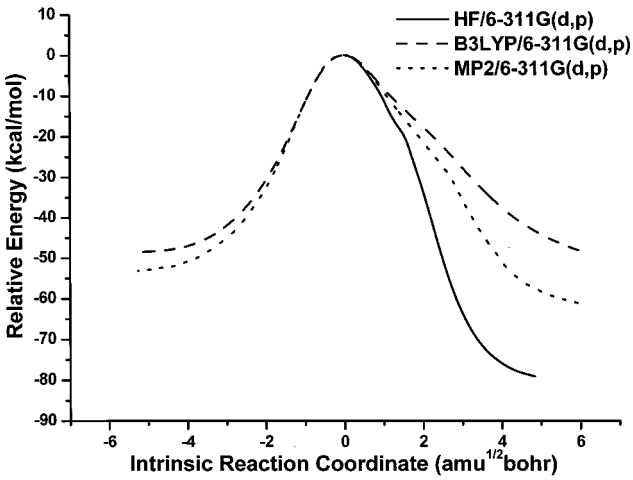

FIG. 2. Potential energy along the reaction path for glyoxal→H_2CO+CO at HF/6-311G(d,p), MP2/6-311G(d,p), and B3LYP/6-311G(d,p).

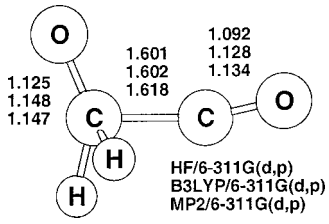

FIG. 3. Molecular geometry at $s=1.5$ amu$^{1/2}$ bohr.

channel. The average translational energies for CO and H_2CO are 17.6 and 16.4 kcal/mol, respectively. As might be anticipated, the CO and H_2CO translational energy distributions have similar profiles, since the velocity distribution is fixed by conservation of linear momentum. In the experimental photodissociation of glyoxal, even though two CO's are produced from each $C_2H_2O_2 \rightarrow H_2+2CO$ three-body dissociation, more than half of the CO produced comes from the $C_2H_2O_2 \rightarrow H_2CO+CO$ channel because of its higher branching ratio (65%).[9] The HCOH+CO channel has a much lower branching ratio (7%), and, by comparison with the other two channels, does not contribute significantly. The average translational energy for CO from the three-body dissociation channel is 7.4 kcal/mol. Using the branching ratio from the experiment, the combined translational energy of CO is calculated to be 13 kcal/mol, compared to the experimental value of 15 kcal/mol.[9]

Figure 5 shows the vibrational population distribution of CO obtained from the present trajectory calculations. It is particularly interesting that the CO from the H_2CO+CO channel is produced with almost no vibrational excitation (0.98 ± 0.01 in $v=0$). In light of the transition structure shown in Fig. 1(c), this seems reasonable since the CO bond length is very close to that of the product equilibrium structure. By comparison, the CO from the "triple whammy" channel has a population of 0.11 in $v=1$ at the B3LYP/6-311G(d,p) level of theory. Consequently, the combined vibration distribution for CO is 0.94 in $v=0$, which is in good accord with experiment, where the CO($v=1$)/CO($v=0$) ratio was estimated to be less than 0.05.[10]

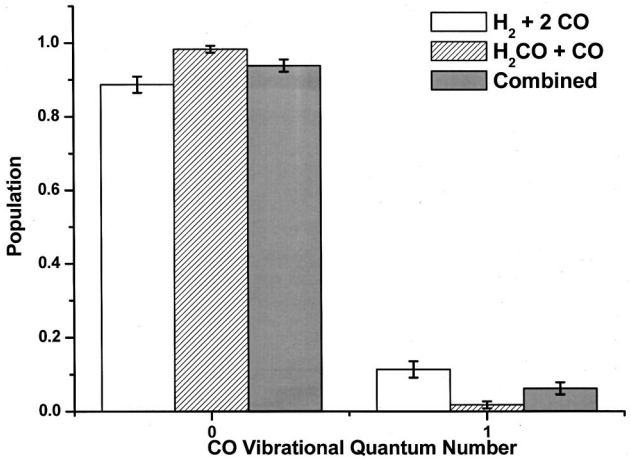

FIG. 5. Vibrational populations for CO computed at B3LYP/6-311G(d,p).

The rotational state distribution of the CO product is presented in Fig. 6. The distribution for the H_2CO+CO channel is significantly broader and has a higher average J than for the H_2+2CO channel. By assuming a symmetric breakup with a planar transition state geometry for the three-body dissociation, Burak and co-workers deduced that this channel would not produce high J CO products.[10] However, our earlier calculations[13] for the triple whammy channel show that the breakup starts asymmetrically from a nonplanar C_2 transition structure. The combined CO rotational distribution obtained from the trajectory calculations is in very good agreement with experiment,[10] yielding a broad distribution with a maximum near $J=40$, compared to the experimentally observed maximum at $J=42$. The calculations also show that the rotational distribution for H_2CO is very broad, ranging up to $J=85$, with an average value of $\langle J\rangle=50.3$, and corresponds to a rotational energy of 10.9 kcal/mol.

Table IV compares the vibrational state distributions of H_2CO for different normal modes. The calculations show an average vibrational energy of 6.3 kcal/mol above the zero point vibration for H_2CO. Modes 1, 2, 3, and 4 are significantly excited, corresponding to the out-of-plane bending, CH_2 rocking, CH_2 scissoring, and CO stretching modes.

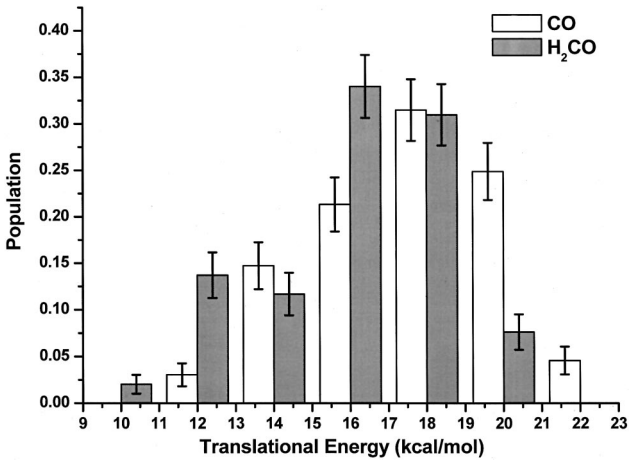

FIG. 4. Translational distribution for H_2CO and CO products.

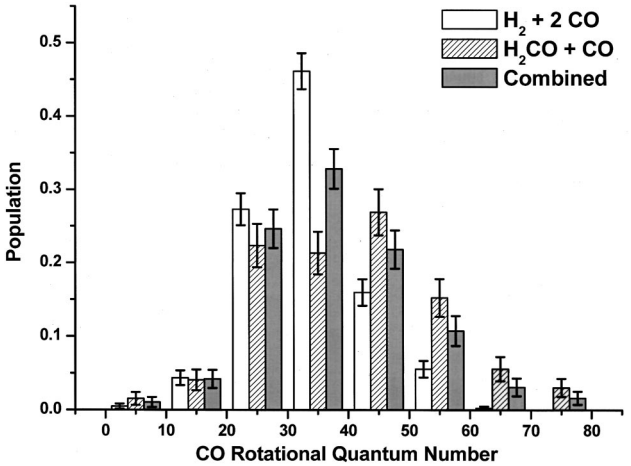

FIG. 6. Rotational populations for CO computed at B3LYP/6-311G(d,p).

TABLE IV. H_2CO product vibrational states distribution.

Mode assignment	Zero point frequency[a]	Vibrational quantum number $v=0$	$v=1$	$v=2$	$v=3$	$v=4$	$v=5$
Out-of-plane bend	1202	65.8	25.4	7.5	0.9	0.4	
CH_2 rock	1270	42.5	33.8	10.5	11.4	1.3	0.4
CH_2 scissor	1539	55.7	34.6	8.3	1.3		
CO stretch	1827	61.8	30.7	7.0	0.4		
Symm. CH stretch	2869	90.8	9.2				
Asymm. CH stretch	2918	99.1	0.9				

[a]Harmonic frequencies in cm^{-1} without scaling.

The partitioning of the available energy obtained from the trajectory calculation for the H_2+2CO and H_2CO+CO channels are summarized in Table V. The available energy was calculated as the sum of the excitation energy of 0_0^0 band and the heat of reaction. In the three-body dissociation channel, the available energy partitioned into H_2 and 2 CO translations were calculated to be 43.4% and 23.4%, respectively, compared to the experimental partitioning of 46.8% ($v=1$ only) and 22.4%. In the H_2CO+CO channel, translation and rotation account for about 82.7% of the available energy. As might be anticipated, the CO and H_2CO products have comparable amount of energies in translation and in rotation, because of the similar moments of inertia and the conservation of linear and angular momentum. Most of the vibrational energy goes to H_2CO vibrational excitations, since CO bond length in the transition state is already very close to its equilibrium value.

IV. CONCLUSION

In this work, *ab initio* classical trajectory studies were carried out for the glyoxal photodissociation via $C_2H_2O_2 \rightarrow H_2CO+CO$ at the B3LYP/6-311G(d,p) level of theory. When combined with our previous study on the glyoxal three-body fragmentation, the overall vibrational and rotational distributions of CO product are in excellent agreement with the experimental observations. The calculated vibrational energy distribution for H_2CO predicts significant excitation for a number of the normal modes. The rotational distribution of H_2CO is computed to be very broad, ranging up to $J=85$, with $\langle J \rangle = 50.3$. When the H_2+2CO and $CO+H_2CO$ channels are combined, the average translational energy for CO is in very good agreement with experiment.

TABLE V. Average partitioning of available energy.

Product	Mode	Calculated % energy disposal	Expt. % energy disposal
$C_2H_2O_2 \rightarrow H_2+2CO$ channel			
H_2	rotation	2.8	3.1[a]
	vibration	6.1	17.8[a]
	translation	43.4	46.8[a]
2CO	rotation	22.1	9.9[c]
	vibration	2.2	0.0[b]
	translation	23.4	22.4[b]
$C_2H_2O_2 \rightarrow H_2CO+CO$ channel			
CO	rotation	15.2	
	vibration	0.1	
	translation	26.5	
H_2CO	rotation	16.5	
	vibration	17.2	
	translation	24.5	

[a]Reference 12.
[b]Reference 9.
[c]Reference 10.

ACKNOWLEDGMENTS

This work was supported by grants from the National Science Foundation (CHE 9874005 and CISE 9977815). The authors would like to thank William L. Hase for helpful discussions, and Wayne State University for computer time.

[1] R. A. Beyer, P. F. Zittel, and W. C. Lineberger, J. Chem. Phys. **62**, 4016 (1975).
[2] G. H. Atkinson, M. E. McIlwain, and C. G. Venkatesh, J. Chem. Phys. **68**, 726 (1978).
[3] B. G. MacDonald and E. K. C. Lee, J. Chem. Phys. **71**, 5049 (1979).
[4] R. Naaman, D. M. Lubman, and R. N. Zare, J. Chem. Phys. **71**, 4192 (1979).
[5] G. W. Loge, C. S. Parmenter, and B. F. Rordorf, Chem. Phys. Lett. **74**, 309 (1980).
[6] G. W. Loge and C. S. Parmenter, J. Phys. Chem. **85**, 1653 (1981).
[7] Y. Osamura, H. F. Scheafer, M. Dupuis, and W. A. Lester, J. Chem. Phys. **75**, 5828 (1981).
[8] Y. Osamura and H. F. Schaefer, J. Chem. Phys. **74**, 4576 (1981).
[9] J. W. Hepburn, R. J. Buss, L. J. Butler, and Y. T. Lee, J. Phys. Chem. **87**, 3638 (1983).
[10] I. Burak, J. W. Hepburn, N. Sivakumar, G. E. Hall, G. Chawla, and P. L. Houston, J. Chem. Phys. **86**, 1258 (1987).
[11] G. E. Scuseria and H. F. Schaefer, J. Am. Chem. Soc. **111**, 7761 (1989).
[12] L. M. Dobeck, H. M. Lambert, W. Kong, P. J. Pisano, and P. L. Houston, J. Phys. Chem. A **103**, 10312 (1999).
[13] X. Li and H. B. Schlegel, J. Chem. Phys. **114**, 8 (2001).
[14] D. M. Koch, N. N. Khieu, and G. H. Peslherbe, J. Phys. Chem. A **105**, 3598 (2001).
[15] X. Li, J. M. Millam, and H. B. Schlegel, J. Chem. Phys. **114**, 8897 (2001).
[16] W. L. Hase, in *Encyclopedia of Computational Chemistry*, edited by P. v. R. Schleyer, N. L. Allinger, T. Clark, J. Gasteiger, P. A. Kollman, H. F. Scheafer III, and P. R. Schreiner (Wiley, New York, 1998), p. 402.
[17] G. H. Peslherbe, H. Wang, and W. L. Hase, in *Monte Carlo Methods in Chemical Physics*, edited by D. M. Ferguson, J. I. Siepmann, and D. G. Truhlar (Wiley, New York, 1999), Vol. 105.
[18] M. J. Frisch, G. W. Trucks, H. B. Schlegel *et al.*, GAUSSIAN 98, Gaussian, Inc., Pittsburgh, PA.
[19] V. Bakken, J. M. Millam, and H. B. Schlegel, J. Chem. Phys. **111**, 8773 (1999).
[20] C. Gonzalez and H. B. Schlegel, J. Chem. Phys. **90**, 2154 (1989).
[21] C. Gonzalez and H. B. Schlegel, J. Phys. Chem. **94**, 5523 (1990).

[22] M. C. Gutzwiller, *Chaos in Classical and Quantum Mechanics* (Springer-Verlag, New York, 1990).
[23] W. L. Hase, in *Encyclopedia of Computational Chemistry*, edited by P. v. R. Schleyer, N. L. Allinger, T. Clark, J. Gasteiger, P. A. Kollman, H. F. Scheafer III, and P. R. Schreiner (Wiley, New York, 1998), p. 399.
[24] X. Li, J. M. Millam, and H. B. Schlegel, J. Chem. Phys. **113**, 10062 (2000).
[25] R. A. Fletcher and G. Pilcher, Trans. Faraday Soc. **66**, 794 (1970).